Journal of Environmental Economics & Chemical Processes (JEECP)

https://doi.org/10.22034/jeecp.2025.735015

Journal homepage: *WWW.JEECPJournal.com*

Journal of Environmental Economics & Chemical Processes (JEECP)

ORIGINAL RESEARCH PAPER

Comparison of the Impact of NPC and Alumina/Silica Nano Hybrid Emulsion on CEOR

Abbas Khaksar Manshad*, Younes Sharifiyan, Siyamak Moradi

Department of Petroleum Engineering, Abadan Faculty of Petroleum, Petroleum University of Technology (PUT), Abadan, Iran.

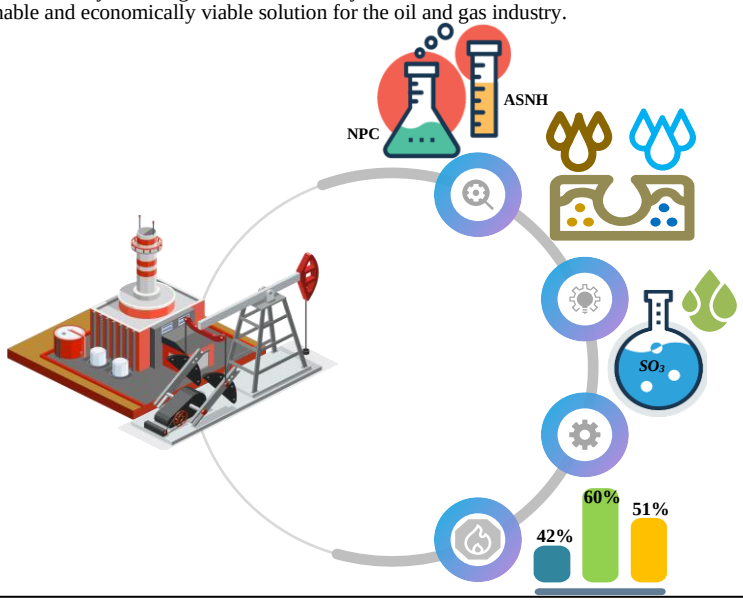
P A P E R I N F O

Paper history:
Received 10/15/2025
Accepted in revised form12/25/2025

***Keywords*:**
Smart Water
Interfacial Tension (IFT)
Nanocomposites
Chemical Enhanced Oil Recovery
Nano Hybrid Emulsion

A B S T R A C T

This study delves into the potential benefits of utilizing smart waterflooding as a method for improving oil recovery in carbonate reservoirs. Unlike traditional methods that rely on costly or hazardous chemicals, this approach employs the use of nanoporous carbon (NPC) and alumina/silica nanohybrid emulsion (ASNHE) to investigate their impact on interfacial tension (IFT) and wettability alteration on carbonate reservoir rocks from Asmari formation, as well as their combined synergistic effects on oil recovery. The research found that increasing the concentration of sulphate up to four times in the presence of other ions resulted in the most significant alteration of rock wettability towards water-wet. This suggests that smart waterflooding has the potential to be an effective method for improving oil recovery without the need for expensive or hazardous chemicals. Additionally, the study revealed that the use of ASNHE significantly reduced the oil/water IFT, resulting in a notable increase in oil recovery. Specifically, the use of seawater flooding resulted in a 42% increase in oil recovery, while SW4S+NPC and SW4S+ASNHE flooding resulted in an increase of 60% and 51%, respectively. Overall, the findings of this research paper suggest that the use of smart waterflooding, combined with NPC and ASNHE, has the potential to be a promising approach for improving oil recovery in carbonate reservoirs. By reducing the need for costly and hazardous chemicals, this method could provide a more sustainable and economically viable solution for the oil and gas industry.



1. Introduction

Carbonate reservoirs contain over half of the world's remaining oil [1]. However, they are some of the most complex reservoirs to characterize, manage, and model due to their low primary oil recovery. Nevertheless, their potential for enhanced oil recovery is high. Many of these reservoirs have very low permeability and are thought to be intermediate oil-wet, making the challenge of enhanced oil recovery from them even more important.

Enhanced oil recovery (EOR) refers to any method used to produce oil that goes beyond relying on natural reservoir pressure. The choice of a suitable EOR method depends on various factors, including economic and technological considerations. Typically, EOR methods are applied after secondary recovery operations, and the goal is to recover about 45% of the original oil in place (OOIP) [2]. In addition, primary and secondary recovery methods can recover approximately one-third of the OOIP.

* Corresponding author: Abbas Khaksar Manshad
E-mail address: khaksar@put.ac.ir
ISSN: 3116-0050
URL: https://www.jeecpjournal.com/article_735015.html

Please cite this article as: A. Khaksar Manshad, Y. Sharifiyan, S. Moradi, *Journal of Environmental Economics & Chemical Processes (JEECP)*, 2026, **2(2)**, 21-27.

/© 2026 The Author(s). Published by Institute of Power, Movement, and Innovative Insight

Water-flooding is a secondary recovery method that includes injecting water into an underground reservoir to increase its production. The term "smart water," as well as related terms such as "engineered water," "advanced ion management," and "low salinity water," refer to methods of altering the ion concentrations in water to increase beneficial ions and decrease harmful ones. This can involve diluting or purifying saline samples to reduce overall salinity, as well as making other changes to the water chemistry. The primary goal of using smart water is to modify the wettability of surfaces, with the impact of salinity on interfacial tension (IFT) still not fully established. The effects may vary depending on the conditions of the system being studied, including the composition of the crude oil and the thermodynamic environment. The use of different brine formulations can also influence whether IFT is increased or decreased. In some cases, it may be more cost-effective to treat and control the ion concentration in available water rather than transporting water with lower salinity to the field. This approach may be particularly useful when access to water is limited or difficult.

The reduction of IFT between the oil and the injected fluid is a crucial and efficient EOR mechanism. IFT is a measure of energy at the interface of two immiscible fluids. The IFT value is a measure that shows the miscibility of fluids in the reservoir; the lower the IFT value, the closer the fluids are to miscibility. A fully miscible fluid state is indicated by an IFT value of 10-3 mN/m, which is considered ultra-low. Under standard conditions, the average IFT value between oil and water is 10-30 nM/m. Immiscible behavior between fluids and the prevention of oil displacement from the reservoir is caused by a high IFT value between oil and water. The extraction of oil trapped in the reservoir's pore network becomes easier by reducing the IFT, which decreases the capillary pressure. In EOR processes, nanofluids, surfactants, polymers, and low-salinity water tend to reduce IFT and are successful agents.

The utilization of nanotechnology for enhanced oil recovery (EOR) has demonstrated its effectiveness in reducing interfacial tension (IFT). Nanofluids, also known as smart nanofluids, are used for this purpose. Nanoparticles, which are small particles ranging from 1 to 100 nanometers, possess unique chemical and physical properties that make them significant in EOR. Their high surface area allows for a strong driving force for diffusion, particularly at high temperatures. Additionally, their small size enables them to easily pass through the pore throat of a porous medium. The use of nanoparticles in EOR has resulted in favorable outcomes such as IFT reduction, wettability alteration, asphaltene inhibition, viscosity reduction of oil, viscosity enhancement of injecting fluid, disjoining pressure, pore channel plugging, and nano-emulsion creation. Numerous research studies have reported that nanoparticles play a crucial role in chemical enhanced oil recovery (CEOR) processes. The NEOR method commonly employs chemical methods such as smart water, surfactants, polymers, gas, and carbonated injection in combination with hybrid nanocomposites to enhance the performance of the CEOR process. Ultimately, this combination of techniques can increase the potential for wettability alteration and reduce IFT in EOR.

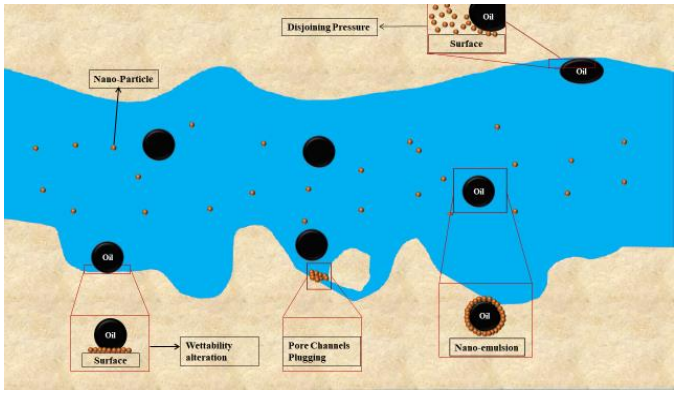


Figure 1. The schematic of the EOR mechanisms of nanofluids.

Some recent studies on application of nanoparticles in Enhanced Oil Recovery Hendraningrat et al. studied the possibility of using SiO_2 nanofluids for EOR in sandstones (9–400 mD) and concluded that the SiO_2 nanoparticles are proper for EOR in water wet sandstone [3]. An investigation on the effect of different nanofluids of Calcium carbonate ($CaCO_3$), Zirconium dioxide (ZrO_2), Silicon dioxide (SiO_2), Titanium dioxide (TiO_2), Aluminum oxide (Al_2O_3), Magnesium oxide (MgO), Carbon nanotube (CNT) and Cerium oxide (CeO_2) on the wettability of carbonate rocks [4]. According to results of contact angle measurements at non-aged sample θ=145° means that the sample was oil wet after measurements θ equals 63.5 °, 60°, 64°, 49.5°, 58°, 99°, 103°, and 107.5° for ZrO_2, $CaCO_3$, CNT, TiO_2, SiO_2, MgO, Al_2O_3 and CeO_2 respectively. So $CaCO_3$, TiO_2 and SiO_2 were the most effective nanoparticles. Le at al studied synergistic blends of SiO_2 nanoparticles and surfactants for EOR in high-temperature reservoirs. They conducted tests combining different types of surfactants with SiO_2 nanoparticles. Some of the blends showed great potential for EOR application due to their resistance to adsorption onto the rock surface, and thermostability at 91°C, extremely good in brine-crude oil interfacial tension reduction and very high oil displacement efficiency [5]. Zirconium-oxide (ZrO_2) based nanofluids influence on wettability modification of limestone formation through contact angle measurement. Initial contact angle measurement carried out with distilled water as benchmark, for a drop water in air was 92° and for a drop of water in toluene was 152°. Then oil wet calcite substrate exposed to ZrO_2 and at suitable nanoparticle concentration wettability altered from neutral network (92°) to weakly water-wet (64°) for water drop in air, however for water drop in toluene from strongly oil wet (152°) to intermediate wet (89). So this research conclude that ZrO_2 nanofluid can be an effective agent for enhanced oil recovery through wettability modification [6]. TiO_2, SiO_2 and CNT (carbon nanotube) nanofluid for enhanced gas recovery by wettability modification from liquid wetting to ultra-gas wetting of carbonates, results in improving the well's deliverability. As the rock wettability was altered to gas wetting condition the water contact angle increased to 161°, 164°, and 163° also for n-decane (as oil phase) increased to 144°, 151°, and 147° when rock aged in TiO_2, SiO_2 and CNT respectively [7]. What sets this research apart is that it is the first time a SiO_2/Al_2O_3 nanohybrid emulsion and NPC has been tested on Asmari Formation rock. This represents a significant advancement in the field, as it provides new insights into the potential of using these nanoparticles for enhanced oil recovery in this specific geological formation.

Table 1. A summary of some previous works on effects of nanoparticles on contact angle.

NPs	Porous Media	Contact angle		Ref.
		Without NPs	With NPs	
$CaCO_3$	Carbonate rock	145°	60°	[4]
ZrO_2	Carbonate rock	145°	63.5 °	[4]
(TiO_2)	Carbonate rock	145°	49.5°	[4]
(Al_2O_3)	Carbonate rock	145°	103°	[4]
(MgO),	Carbonate rock	145°	99°	[4]
(CNT)	Carbonate rock	145°	64°	[4]
SiO_2	Carbonate rock	145°	58°	[4]
CeO_2	Carbonate rock	145°	107.5°	[4]
Al_2O_3	Carbonate rock	85°	62°	[8]
ZrO_2	Limestone	152°	89°	[6]
TiO_2	Limestone	90°	46°	[9]
SiO_2	Sandstone	135.5°	66°^{17}	[4]
NSP	Sandstone	166°	130°	[10]
CNP	Sandstone	166°	124°	[10]
Al_2O_3	Sandstone	131o	92o	[11]
Fe_2O_3	Sandstone	132.5°	101°	[11]
SiO_2	Sandstone	134°	82°	[11]

Table 2. A summary of some previous works on effects of different types of nanoparticles on IFT.

	Material Type	Outcome	Reference
Metal oxide Based	ZnO	the IFT was reduced by up to 50%.	[12]
	Tio_2	The IFT was reduced by up to 22.2%	[13]
Carbon Based	Graphene oxide (GO)	The IFT was reduced by up to 36.3%	[14]
	Multi-walled carbon nanotubes (MWCNTs)	The IFT was reduced by up to 47%	[13]
Polymer Based	Sulfonated polystyrene nano-particles (SPNPs)	The IFT was reduced by up to 90%	[15]
	Polyvinylpyrrolidone (PVP)	The IFT was reduced by 60%	[16]
Lipid-Based	Solid lipid nanoparticles (SLNs)	The interfacial tension was reduced by 41.8%	[13]
Magnetic Based	Iron oxide (Fe_3O_4)	IFT reduction by up to 90%	[17]

2. Method

➢ Oil phase and Aqueous Phase

In this research, the crude oil of Ahwaz oilfield was used and its properties are shown in Table 3. distilled water was the aqueous phase in order to conduct for smart water/Nano fluids solutions and also core flooding tests.

Table 3. Physical properties of oil sample.

Viscosity (cP)	Density (gr/cc)	Gravity (°API)
13.23	0.878	32.6

➢ Salts

Table 2-2 shows the salts used for making the smart water in this study provided by the German Merck Company with a purity higher than 99%.

Table 4. Salts used in smart water solutions.

Salt	Chemical Formula
Sodium Chloride	NaCl
Magnesium Chloride Hexahydrate	$MgCl_2.6H_2O$
Sodium Bicarbonate	$NaHCO_3$
Calcium Chloride Dehydrates	$CaCl_2.2H_2O$
Sodium Sulfate	Na_2SO_4

Table 5. A mount of used salts to synthesize brine solutions.

Salts	SW	SW2S	SW4S	SW2C	SW4C	SW2M	SW4M
$MgCl_2.6H_2O$	12.16	12.16	12.16	12.16	12.16	24.318	48.636
$CaCl_2.2H_2O$	1.177	1.177	1.177	2.355	4.708	1.177	1.177
Na_2So_4	4.8	9.61	19.22	4.8	4.8	4.8	4.8
$NaHCO_3$	0.23	0.23	0.23	0.23	0.23	0.23	0.23
NaCl	31.5	33.48	25.65	36.52	34.65	30.56	16.53

➢ Synthesize of nanomaterials

Nanoporous Carbon (NPC) and Alumina/Silica Nanohybrid Emulsion (ASNHE) were used in this study which both were synthesized in Research Institute of Petroleum Industry. Hydrothermal process was employed to synthesize these nanomaterials. Properties of two nanomaterials are shown in Table 6.

Table 6. Properties of nanomaterials.

Nanostructure	Shape of Nanoparticles	Approx-size (nm)	Molecular weight (gr/mol)
Nanoporous Carbon (NPC)	Spherical	8-15	59.86
Alumina/Silica Nanohybrid Emulsion (ASNHE)	Spherical	7.5-15	50.08

2.1. Methodology

2.1.1. Characterization of ASNHE Nanocomposite

X-Ray Diffraction (XRD), Transmission Electron Microscopy (TEM), scanning electron microscope (SEM) analytical approaches are techniques used in materials science to determine the crystallographic structure of a material, its functional groups, and surface morphology. XRD works by irradiating a material with incident X-rays and then measuring the intensities and scattering angles of the X-rays that leave the material. TEM is a microscopy technique in which a beam of electrons is transmitted through a specimen to form an image. An image is formed from the interaction of the electrons with the sample as the beam is transmitted through the specimen. SEM is used to obtain high-resolution images of a sample's surface morphology by scanning it with a focused beam of electrons.

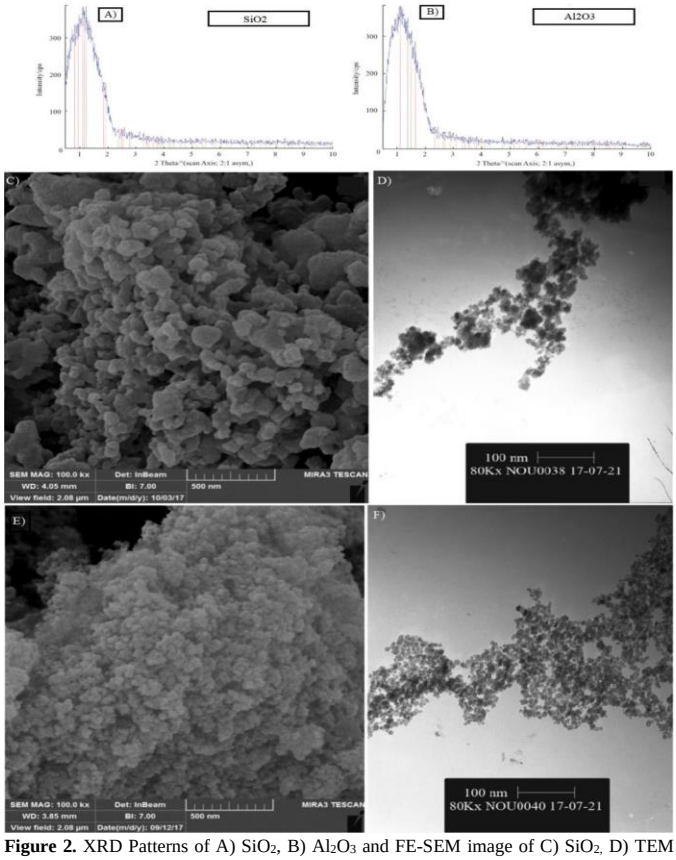


Figure 2. XRD Patterns of A) SiO_2, B) Al_2O_3 and FE-SEM image of C) SiO_2, D) TEM image of SiO_2, E) FE-SEM image of Al_2O_3, F) TEM image of Al_2O_3 [18].

The XRD pattern of SiO_2 shows a sharp peak at $2\theta = 26.6°$, which is characteristic of the (100) plane of quartz. This peak indicates that the SiO_2 is crystalline and has a high degree of crystallinity. The absence of other peaks indicates that the SiO_2 is not contaminated with other phases.

The XRD pattern of Al_2O_3 shows sharp peaks at $2\theta = 37.7°$, 43.8°, 52.5°, 57.4°, 66.5°, and 68.1°. These peaks are characteristic of the (100), (002), (110), (111), (200), and (220) planes of α-Al_2O_3. The presence of these peaks indicates that the Al_2O_3 is crystalline and has a high degree of crystallinity. The absence of other peaks indicates that the Al_2O_3 is not contaminated with other phases.

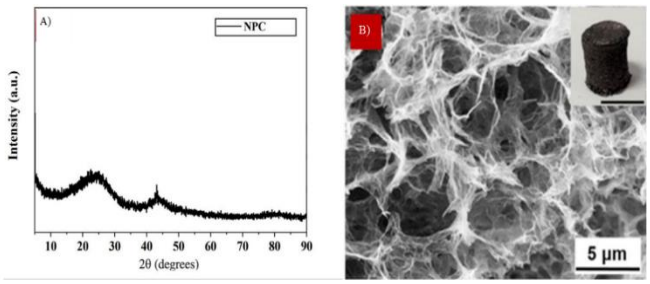


Figure 3. A) XRD pattern of NPC, B) SEM image of NPC.

It is found that NPC exhibit two broad and low-intensive diffraction peaks centered at $2\theta = 20°–26°$ and 43°–44°, clearly indicating an amorphous nature and low graphitization degree of the nanoporous carbon materials.

2.2. Density, Conductivity and pH Measurements

The density of solutions used in the measurements must be determined. The density was measured using a DA-640 density meter made by KEM Company. Additionally, the JENWAY model 4510 conductivity meter was utilized in this research to measure the CMC of the surfactant solutions.

The JENWAY model 4510 conductivity meter is a commonly used conductivity meter in laboratory settings. It has a conductivity range of 0 to 199.9µS and a resolution of 0.1µS. The model 4510 has an accuracy of ±0.5% ± 2 digits [19].

2.3. IFT Measurement

The pendant drop method was utilized to conduct IFT measurements between oil and various types of solutions. A VIT-6000 device (manufactured by Fars, with a 99% accuracy) was employed, consisting of ISCO pumps, a chamber with glass windows, a closed metal needle at the bottom of the chamber, a light projection, a camera, and a computer with image processing software. This software was utilized to determine the IFT value under both static and dynamic conditions. To measure IFT between two liquids, a drop of crude oil was suspended from the needle in the presence of the solution filled in the main chamber. The crude oil drop was controlled by an ISCO pump (Teledyne ISCO, Model D - 500, pressure accuracy 0.1%). Images of oil droplets were recorded at various time stages with a digital camera. The software calculated the IFT between oil droplets and aqueous solution according to Eq. (1), Fig. 5 illustrates this device.

$$\gamma = \frac{gDe^2\Delta\rho}{H} \quad (1)$$

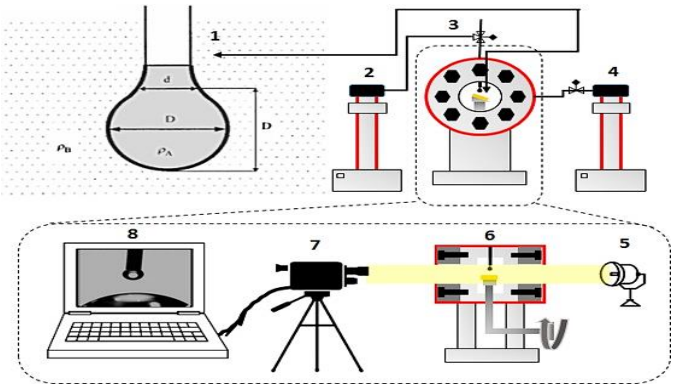


Figure 4. Illustration of IFT setup, (1) Illustration of digital drop of liquid shape (crude oil in this case), (2) ISCO pump for controlling crude oil droplet, (3) Main chamber for the IFT measurement, front view, (4) ISCO pump for filling the main chamber with fluid, (5) Light projection, (6) Main chamber, side view, (7) Video camera for recording, (8) computer software for interpretation [12].

As all tests in this study were conducted at ambient pressure and temperature, both the electrical heaters and pressure transmitter were programmed to be turned off.

2.4. Ultrasonic Agitation System

Nanofluids are a type of fluid that contain suspended nanoparticles, and they have shown promise in a variety of applications due to their unique properties. In this study, nanofluids were prepared by sonication of dispersed nanoparticles in a smart water solution. The dispersion was vigorously agitated using a UP200H Ultrasonic homogenizer for a total of 2 hours, which was spread across eight periods at 15 minute intervals. To ensure adequate homogeneity and avoid overheating, there was a five-minute break between each interval. The sonication process is an effective method for dispersing nanoparticles in a liquid medium, and the use of smart water solution as a base fluid enhances the stability and heat transfer properties of the nanofluids. The resulting nanofluids can have potential applications in various fields such as electronics, energy, and biomedical engineering. Further investigations are needed to explore their full potential.

2.5. *Dynamic Flooding Experiment*

After preparing the core plug, it was saturated with brine through vacuum pump in order to start flooding. It was placed in the rubber sleeve, which was used as a connection to exert overburden pressure on the rock in the core holder. In these experiments, the overburden pressure was around 2500 psi. The outlet valve of the coreflood system was closed and the inlet valve and transfer vessel related to brine accumulator were opened. All these were done to make sure that the plug was saturated completely with brine by a vacuum pump, and to minimize the possible experimental errors caused by the core exposure to air due to displacing core from vacuum pump to core holder. Then, about one or two pore volumes of brine were flooded (First flood).

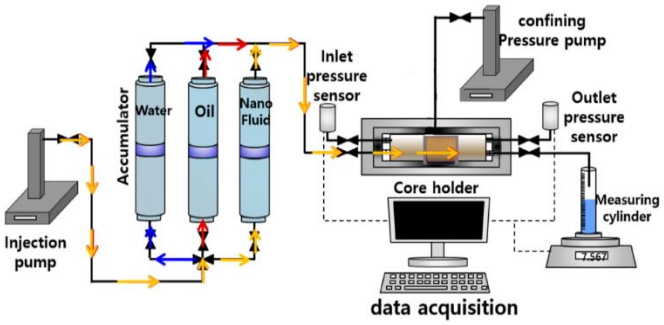


Figure 5. Core flood apparatus.

Next, the transfer vessel changed, so oil accumulator valve was opened (second flood), and the injection of oil was continued until no water was detected at the outlet (that is the core plug reaches S_{wi}). The volume of discharged water was measured and the S_{wi} was calculated. The dead volume of core holder and lines (about 9 cc) was calculated and subtracted from the output water to find out the percentage of the initial water saturation in the core plug.

2.6. Experimental Methods

First Solid pellets (1cm diameter and 4mm thickness) were prepared from the plug using core cutting machine.in order to synthesize brine solutions, deionized water and five main salts include $MgCl_2.6H_2O$, NaCl, $NaHCO_3$, $CaCl_2.2H_2O$ and Na_2SO_4 were mixed in the volumetric balloon, Nanofluids were prepared by sonication of dispersed nanoparticles in smart water solution. After cleaning and drying, the core sample was saturated. flask and vacuum made by specific pump. After one hour, while the pump was still working, the funnel's valve opened and the sample plug was immersed in brine. The plug was saturated with brine with 100000 ppm NaCl, for at least 24 hours to establish initial condition of the plug.

When the pellets cleaned with toluene in Soxhlet extractor, they were immersed in the crude oil from Ahwaz and were put in average 80°C temperatures for at least 100 hours. Then, the pellets were cleaned with a little Kerosene. After all these steps, the pellets were oil wet enough to perform the wettability alteration tests.

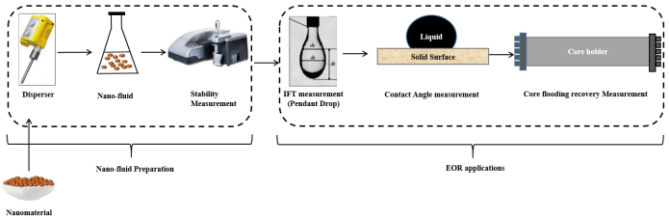


Figure 6. Experimental procedures taken in this study.

3. Results and Discussion

This section presents the results of the conducted tests. At the first step the cores are characterized for determining the dimension, pore volume, permeability, porosity and other properties. In the next section, DLS test results were determined. In section 3.3 CMC of NPC and ASNHE were determined by conductivity and pH tests. Section 3.4 shows the results of IFT measurements by using pendant drop method. In section 3.5 the results of carbonate pellets wettability alteration were showed. Lastly, section 3.6 shows results of core flooding tests.

Characteristics of core plugs are presented in Table 7 Both core samples were taken from Carbonate Reservoir Rocks from Asmari formation and were aged in heavy oil for seven days and dried in oven for 72 hours to prepare strongly oil-wet samples. The entire data of the flow rate and pressure differences and their curves for calculating liquid permeability are shown in Figures 7.

Table 7. Characteristics of core plugs.

Sample ID	C-1	C-2
Length (cm)	7.2	7.7
Diameter (cm)	3.7	3.7
Bulk volume (cc)	71.65	79.89
Dry weight (gr)	191.73	193.71
Saturated weight (gr)	202.56	206.43
Pore volume (cc)	10.16	11.94
Porosity (%)	14.18	14.94
Permeability (mD)	9.88	10.31
OOIP (cc)	6.9	7.8
S_{wi} (%)	32%	34.67

3.1. Nano Silica DLS Test

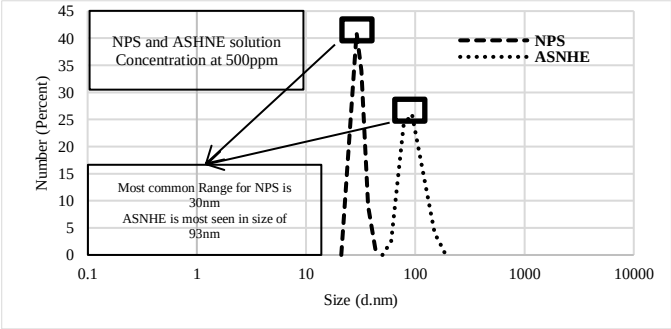


Figure 7. Size Distribution Comparison for NPC and Silica.

Figure 7 shows the results of the size distribution for NPS and Silica solution at concentration of 500 ppm after 24 hours of solutions preparation. According to this chart, the NPS particle size is between 20 and 45 nm, which is most common in the range of 30 nm and the ASNHE particle size is between 50 and 110 nm, which is most common in the range of 93 nm.

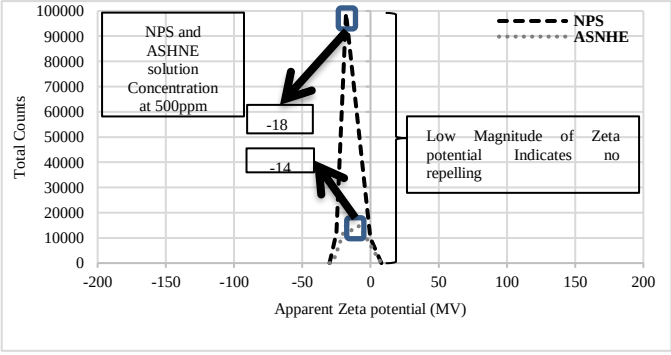


Figure 8. NPS and ASNHE Zeta Potential Curve Comparison After 24 hours.

Figure 8 shows zeta potential curves for NPS and Silica solutions at concentration of 500 ppm. The amount of average zeta potential for NPS

particle is -13.8 which this result indicates the stability of the NPS solution after 24 hours and for Silica is -9.86.

Based on the size distribution and the Zeta potential results, NPC and Silica solutions were still stabilized at 500 ppm concentration after 24 hours of solution preparation.

3.2. Determination of Nanomaterials Critical Micelle Concentration (CMC)

In this work, conductivity method and pH method were implemented to conducting the CMC measurements. At first, several aqueous solution of NPC and ASNHE with concentration 100 ppm to 1500 ppm were prepared.

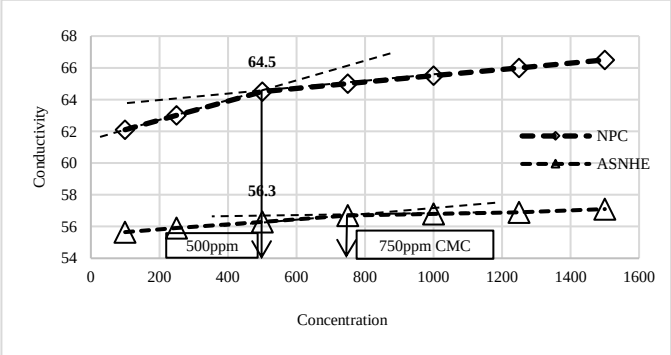


Figure 9. CMC determination, conductivity vs different concentrations of NPC and ASNHE.

Figure 4 shows conductivity versus NPC and ASNHE concentration under 24℃ and 1 atm. As can be seen from the Figure, Noticing the interactions the CMC value for NPC and ASNHE were determined 500 ppm and 750 ppm, respectively.

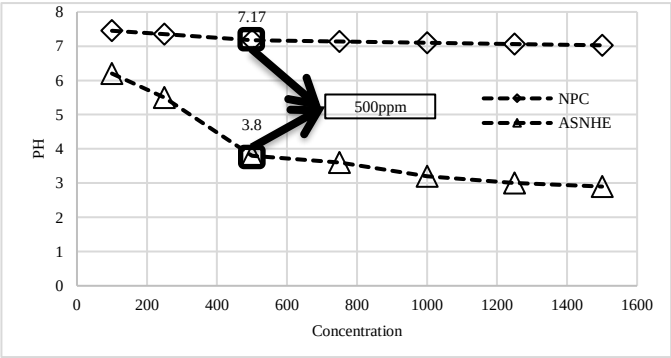


Figure 10. CMC determination, pH vs different concentrations of NPC and ASHNE.

Figure 5 shows pH versus NPC and ASNHE on concentration under 24℃ and 1 atm. The CMC value for both NPC and ASNHE was 500 ppm.

Taking into account the results, the values of 500 ppm and 750 ppm were considered as CMC for NPC and ASNHE, respectively.

3.3. Interfacial Tension Results

As the concentration of NPC and ASNHE in solutions increases, the interfacial tension between the surrounding phase and droplet decreases. This means that the force between the two phases is reduced, allowing for easier mixing and interaction between them

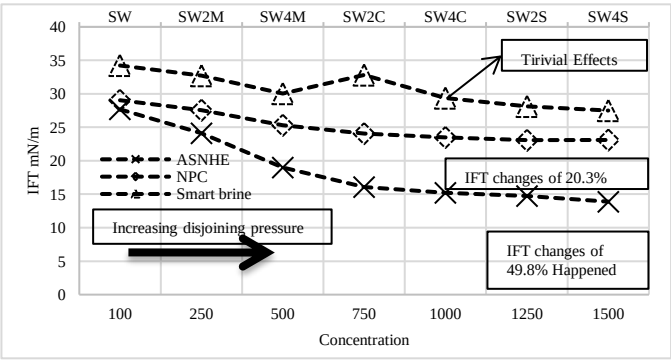


Figure 11. IFT Values at different concentrations.

In experiments, it has been observed that the presence of NPC in solutions has a minimal effect on reducing interfacial tension (IFT) between oil and water. Specifically, the addition of NPC to solutions resulted in a slight decrease in oil/water IFT values from 34 mN/m to 23.12 mN/m. On the other hand, the presence of ASNHE in solutions has been shown to have a significant impact on reducing IFT. The addition of ASNHE to solutions resulted in a substantial decrease in oil/water IFT values from 27.68 mN/m to 13.89 mN/m. It is also worth noting that Smart Brines have been found to have a negligible effect on IFT reduction.

3.4. Contact Angle Measurements

As mentioned earlier, important aims of wettability research are to identify optimum conditions for oil recovery. Contact angle test used as a quantitative wettability test in this work. prepared carbonate pellets were treated with various solutions of smart brines and its combination with NPC and ASNHE. Then, contact angle had measured by a droplet of distillated water in present of kerosene.

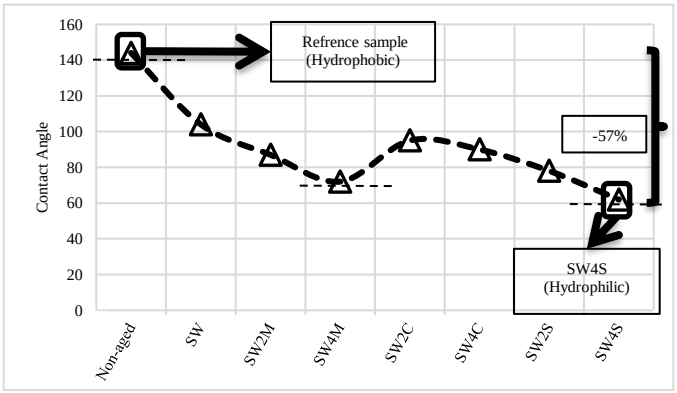


Figure 12. IFT Values at different concentrations.

As shown in Figure 12, the contact angle of a carbonate rock sample before treatment with a solution was measured to be approximately 144°, indicating that the rock is strongly oil-wet. When the rock was treated with seawater (SW), the contact angle was reduced to 104°, demonstrating the effectiveness of seawater in altering the wettability of carbonate rock. Further experiments were conducted to measure the effect of incremental addition of ions on the wettability of the rock. It was found that while increasing the concentration of calcium ions had little effect on wettability, increasing the concentration of magnesium and sulphate ions had a considerable impact. Specifically, treatment with SW4S resulted in a decrease in wettability from 144° to 62°, indicating a significant alteration in wettability.

Further experiments were conducted to investigate the effect of blending seawater with four times the concentration of sulphate (SW4S) with NPC and ASNHE on the contact angle of carbonate rock (as shown in figure 7). It was observed that as the concentration of NPC and ASNHE increased, the contact angle decreased, indicating a change in wettability. Interestingly, it was found that NPC had a greater effect on altering wettability compared to ASNHE.

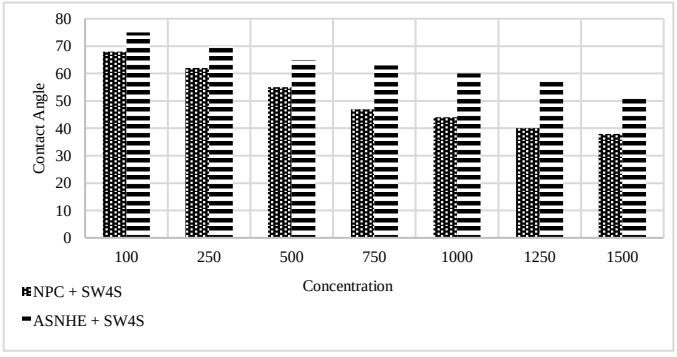


Figure 13. Contact Angle values at different concentrations.

3.5. Core Flooding Results

Two sets of water floods were conducted with the selected solutions as follows:

- **SW4S+NPC flooding**
- **SW4S+ ASNHE flooding**

3.5.1. SW4S+NPC Flooding

Core C-1 was used for this experiment which initial water saturation is 32% and original oil in place is 6.9 cc. Oil recovery due to secondary waterflooding was measured after flooding the synthesized seawater brine into the completely oil saturated carbonate core. Figures 14 and 15 show the oil recovery factor and pressure drop profiles versus pore volume injected, respectively. As depicted in figure 14, the ultimate oil recovery after injecting 1.2 pore volume of seawater is about 41% of initial oil in place (OOIP). As indicated in figure 15 the pressure drop increase moderately until the breakthrough time by injecting seawater. After injection 0.4 pore volume of seawater the pressure drop reaches to 240 psi and then it begins to decrease. After about 1.4 pore volume injection the pressure drop became stable on 178 psi.

After injection 1.4 pore volume seawater, immediately SW4S+NPC (by adding 500 ppm NPS to SW4S) was injected and the output oil from the carbonate plug was recorded. The Figure 16 shows after injection about 1 pore volume SW4S+NPC recovery factor reached 60% and then remains constant. It was observed that 19% of OOIP was recovered due to this treatment.

3.5.2. SW4S+ASNHE

Core C-2 was used for this test which initial water saturation is 34.67% and original oil in place is 7.8 cc. Oil recovery due to secondary waterflooding was measured after flooding the synthesized seawater brine into the completely oil saturated carbonate core. Figures 14 and 15 show the oil recovery factor and pressure drop profiles versus pore volume injected, respectively. As shown in figure 4-15, the ultimate oil recovery after injecting 1.2 pore volume of seawater is about 44% of initial oil in place (OOIP). As shown in Figure 15 the pressure drop increase moderately until the breakthrough time by injecting seawater. After injection 0.3 pore volume of seawater the pressure drop reaches to 222 psi and then it begins to decrease. After about 1.4 pore volume injection the pressure drop became stable on 172 psi.

After injection 1.2 pore volume seawater, immediately SW4S+ASNHE (by adding 750 ppm ASNHE to SW4S) was injected and the output oil from the carbonate plug (C-2) was recorded. The Figure16 shows after injection about 1.3 pore volume SW4S+ASNHE recovery factor reached 51% and then remains constant. It was observed that 7% of OOIP was recovered due to this treatment

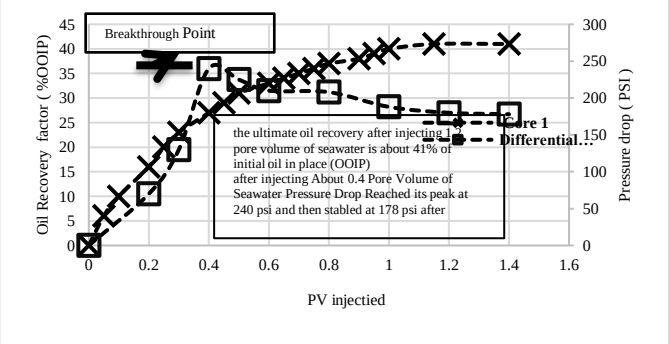


Figure 14. Recovery factor and differential pressure for sea water in core 1.

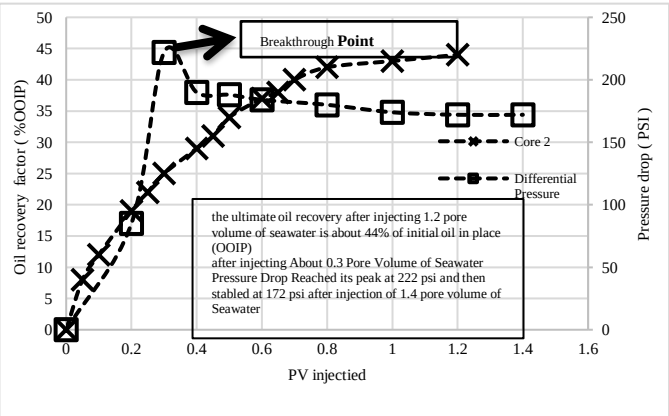


Figure 15. Recovery factor and differential pressure for sea water in core 2.

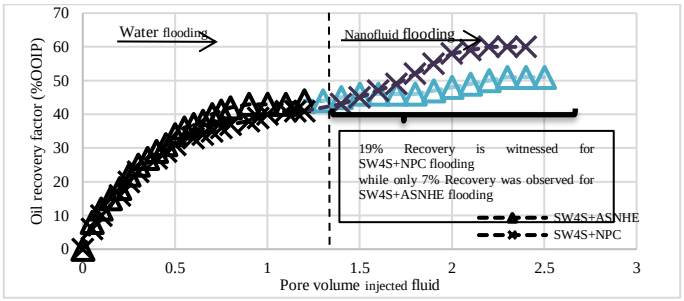


Figure 16. Recovery factor for two different solutions.

3.6. Comparison of Oil Recovery by Selected Fluid Tertiary Flooding

The results of total recovery factor and residual oil of different flooding types are presented in Table 7. As can be seen, the ultimate oil recovery has increased from about 42% in seawater flooding up to 60%, 51% in SW4S+NPC and SW4S+ASNHE flooding, respectively. The results were in agreement with our previous observations in interfacial tension and contact angle measurements where the maximum and minimum recovery factors were for SW4S+NPC and SW4S+ASNHE flooding, respectively.

Table 8. Oil recovery comparison according to RF (%OOIP) and residual oil.

Solutions		RF (%OOIP)	Residual oil saturation
SW4S+NPC	Seawater flooding	41 %	0.4
	Tertiary flooding	60 %	0.271
SW4S+ASNHE	Seawater flooding	44 %	0.366
	Tertiary flooding	51 %	0.212

As mentioned before, by decreasing non–active ions (Cl^- and Na^+) from the injected seawater composition as well as increasing the sulphate (SO_4^{2-}) concentration improves the oil recovery compared to seawater.in SW4S brine, in comparison of the seawater, the amount of sulfate ion has increased four times and also the amount of Cl^-, Na^+, have decreased significantly. In addition, contact angle degree reduced from 104° to 62°. Therefore, the major cause for the increase in oil recovery can be wettability modification of the rock from oil-wet towards water-wet state.

Besides, Addition of NPC and ASNHE to SW4S assist ultimate oil recovery factor. This improvement can be due to the change in the wettability of rock, the reduction of IFT between oil and water and also structural disjoining pressure.

4. Conclusions

In this research, it was attempted to examine the effect of the combination of smart water and two types of nanomaterials on the wettability of carbonate rock. Moreover, the present study investigated the efficiency of solutions in displacing the carboxylic group of oil from the carbonate rock surface and enhanced oil recovery through IFT, contact angle measurement and core flood experiments. In this chapter, the overall conclusions of this study as well as recommendations for future work are presented.

- The wettability measurement results revealed that increasing sulphate concentrations in seawater caused a dominant on rock wettability alteration towards water-wet. Four times sulphate (SW4S) concentrations in seawater seemed to be the optimum sulphate increment that could positively improve oil recovery.
- Unlike wettability measurements results, smart brines had trivial impact on IFT performance.
- Interfacial tension measurements discovered that by increasing NPC concentration from 100 to 1500 ppm, IFT will decline from 29.04 mN/m to 23.12 mN/m and there was not good performance in reducing IFT.
- Interfacial tension measurements discovered that by increasing ASNHE concentration from 100 to 1500 ppm, IFT will decline from 27.68 mN/m to 13.89 mN/m. ASNHE had better performance than NPC and smart brines solutions in IFT reduction.
- In comparison to calcium ion, increasing magnesium ion concentration was more effective in wettability alteration.
- Combining NPC with SW4S favorably decrease the contact angle compared with ASNHE.
- According to contact angle results, SW4S+NPC and SW4S+ASNHE in 1500 ppm concentration had maximum reduction contact angle, but for reducing cost, CMC values (500 ppm for NPC, 750 ppm for ASNHE) were used for core flooding test.

In agreement with contact angle and IFT results, the ultimate oil recovery increased from 42% in seawater flooding up to 60% and 51% in SW4S+NPC and SW4S+ASNHE flooding, respectively.

References

[1] M. Akbar, B. Vissapragada, A. H. Alghamdi, D. Allen, M. Herron, A. Carnegie, D. Dutta, J.R. Olesen, R. D. Chourasiya, D. Logan, D. Stief, (2000). *Oilfield Review*, **12(4)**, 20-21.

[2] S. Thomas, *Oil & Gas Science and Technology - Revue de l'IFP*, 2007.

[3] L. Hendraningrat, S. Li, O. Torsæter, (2013), *Journal of Petroleum Science and Engineering*, 2013, **111**, 128-138.

[4] R. Nazari Moghaddam, A. Bahramian, Z. Fakhroueian, A. Karimi, A. Sharareh, *Energy & Fuels*, 2015, **29**.

[5] Nhu Y, Le & Pham, Duy & Le, Kim & Nguyen, Phuong-Tung. Design and screening of synergistic blends of SiO2 nanoparticles and surfactants for enhanced oil recovery in high-temperature reservoirs. Advances in Natural Sciences: Nanoscience and Nanotechnology. 2, 2011.

[6] L. Nwidee, S. Al-Anssari, A. Barifcani, M. Sarmadivaleh, M. Lebedev, S. Iglauer, *Journal of Petroleum Science and Engineering*, 2016, **149**.

[7] P. Esmaeilzadeh, M. T. Sadeghi, Z. Fakhroueian, A. Bahramian, R. Norouzbeigi, *Journal of Natural Gas Science and Engineering*, 2015, **26**, 1294-1305.

[8] M. S. Moslan, W. R. W. Sulaiman, A. R. Ismail, M. Z. Jaafar, *Chemical Engineering*, 2017, **65 (2017),** 1339-1344.

[9] A. Esfandyari Bayat, R. Junin, A. Samsuri, A. Piroozian, M. Hokmabadi, *Energy Fuels*, 2014, **28**, 6255-6266.

[10] S. Li, O. Torsaeter, The Impact of Nanoparticles Adsorption and Transport on Wettability Alteration of Intermediate Wet Berea Sandstone, *SPE Middle East Unconventional Resources Conference and Exhibition*, 2015.

[11] E. Joonaki, S. Ghanaatian, *Petroleum Science and Technology*, 2014, **32,** 2599-2607.

[12] M. J. Nazarahari, A. Khaksar Manshad, M. Ali, J. A. Ali, A. Shafiei, S. M. Sajadi, S. Moradi, S. Iglauer, A. Keshavarz, Fuel, 2021**, 298**, 120773.

[13] N. M. El-Sherbini, A. A. El-Khodary, M. M. El-Sherbini, *Egyptian Journal of Petroleum*, 2014, **23(2)**, 185-192.

[14] M. A. Hossain, M. K. Alam, M. N. Islam, *Colloids and Surfaces A: Physicochemical and Engineering Aspects*, 2010, **362(1-3)**, 201-207.

[15] S. Carvalho, T. Barros, A. Densy, E. Lachter, S. Regina da Silva. *Colloids and Surfaces A: Physicochemical and Engineering Aspects:* **413(1),** 107-114,

[16] M. A. Al-Dabbagh, A. A. Al-Othman, M. A. Al-Saadi, *Journal of the Saudi Society of Agricultural Sciences*, 2012, **11(1),** 1-8.

[17] M. A. Hossain, M. K. Alam, M. N. Islam, *Physicochemical and Engineering Aspects*, 2010, **362(1-3)**, 201-207.

[18] A. Maleki, B. Sedaee, A. Bahramian, S. Gharechelou, N. Sarlak, A. Mehdizad, M. R. Rasaei, A. Dehghan, *Petroleum*, 2024, **10(2),** 338-353.

[19] JENWAY. *4510 and 4520 Bench Conductivity Meters*. Available from: http://www.jenway.com/product.asp?dsl=248